Indonesian Journal of Electrical Engineering and Computer Science
Vol. 27, No. 2, August 2022, pp. 766~772
ISSN: 2502-4752, DOI: 10.11591/ijeecs.v27.i2.pp766-772

The enhancement of the dual-layer phosphorus configuration in color uniformity and luminous flux of a light emitting diode

Phuc Dang Huu[1], Phung Ton That[2], Phan Xuan Le[3]
[1]Faculty of Fundamental Science, Industrial University of Ho Chi Minh City, Ho Chi Minh City, Vietnam
[2]Faculty of Electronics Technology, Industrial University of Ho Chi Minh City, Ho Chi Minh City, Vietnam
[3]Faculty of Mechanical-Electrical and Computer Engineering, School of Engineering and Technology, Van Lang University, Ho Chi Minh City, Vietnam

Article Info

Article history:

Received Nov 29, 2021
Revised Jun 4, 2022
Accepted Jun 24, 2022

Keywords:

Color rendering index
Lumen efficacy
Mie-scattering theory
Two-layer phosphor
White light emitting diodes

ABSTRACT

A solid-state process was used to generate the green phosphor $Ca_3Si_2O_4N_2:Eu^{2+}$. The luminescence characteristics, dispersed reflection spectra, and heat quenching were investigated initially, followed by the white light emitting diodes (wLED's) manufacture by the Eu^{2+} -stimulated $Ca_3Si_2O_4N_2$ phosphor. Based on the concentration of ion Eu^{2+}, a wide green emission range localized between 510 and 550 nm was seen in Eu^{2+} -doped $Ca_3Si_2O_4N_2$. In $Ca_3Si_2O_4N_2$, the best doping concentration of Eu^{2+} was 1 mol%. An electric multipolar interaction process conveys energy among Eu^{2+} ions, with a necessary conversion distance of around 30.08 Å. Blending a near-ultraviolet (n-UV) light emitting diodes (LED) which has a GaN basis (380 nm) with the blue $BaMgAl_{10}O_{17}:Eu^{2+}$, the green $Ca_3Si_2O_4N_2:Eu^{2+}$, and the red $Ca_3Si_2O_4N_2:Eu^{2+}$ phosphors yielded a wLED with a 88.25 color-rendering indice Ra at 6,029 K correlating color temperature. $Ca_3Si_2O_4N_2:Eu^{2+}$ appears to be a promising option to apply as a converting phosphor in wLED applications.

Corresponding Author:

Phan Xuan Le
Faculty of Mechanical-Electrical and Computer Engineering, School of Engineering and Technology
Van Lang University
Ho Chi Minh City, Vietnam
Email: le.px@vlu.edu.vn

1. INTRODUCTION

White light emitting diodes (WLEDs), a means of illumination has gained their popularities in the past few years due to their outstanding advantages, for instance, consistency, duration, and environmentall friendly [1]–[3]. With such benefits, they are predicted to substitute conventional lighting means in the upcoming years. Blue light emitting diodes (LED) chips coated with $Y_3Al_5O_{12}:Ce^{3+}$(YAG:Ce^{3+}), in yellow color are combined together to generate white light [4]–[6]. Still, the missing of red component in the observable spectra leads to poor color rendering index (CRI) and high color temperature. An alternative method is to mix ultra-violet LED (in the range from 380 to 420 nm) and RGB together. As a result, developing novel phosphors, which are stimulated efficiently in the near ultra-violet region, is a critical possibility that deserves immediate attention [1], [7], [8]. When activated by Eu^{2+}, due to various advantages, such as strong consistency physiccally as well as chemically and bad heat extinguishing, and nitride/oxynitride hosts that created strong luminescence, this substance becomes an ideal for primary materials. Huang *et al.* [9] were the first to publish $Ca_3Si_2O_4N_2$ powder X-ray data. Sharafat described the crystal composition of Ca_3 subsequently. The Ca_3-xSi_2O_4+$2xN_2$-2x [10], [11] luminous characteristics have never been studied earlier. The luminous qualities, heat stability, and utilization of green $Ca_3Si_2O_4N_2:Eu^{2+}$

phosphors in the manufacture of a wLED using a near-ultraviolet (n-UV) LED are all discussed in this paper. The findings reveal that Ca_3Si_2 is thermally stable, and white LEDs made by $Ca_3Si_2O_4N_2:Eu^{2+}$obtain great CRI [12], [13]. The $Ca_3Si_2O_4N_2:Eu^{2+}$-based green phosphor is a viable contender for solid-state lighting sources.

2. EXPERIMENTAL DETAILS

2.1. Characterization of the $Ca_3Si_2O_4N_2:Eu^{2+}$

The $Ca_3Si_2O_4N_2:Eu^{2+}$ polycrystalline phosphorous was made via a solid-state procedure wherein the component unprocessed substances including 99.99% of $CaCO_3$, α-Si_3N_4, Eu_2O_3, and 99.6% of SiO_2, (Aldrich Chemicals, USA) were assessed in stoichiometric proportions. The powder solutions were sintered at 1400 °C in 8 hours in a reduced environment (15%H_2/85%N_2), with a periodic regrinding to avoid undone reaction. The obtained items were subsequently powdered and crushed for more studies after cooling in the oven till reaching room temperature. Bruker AXS D8 innovatory automated diffractometer which has Cu-*Kα* radiation with λ=1.5418 Å, functioning at 40 kV and 30 mA, was used to perform powder x-ray diffraction (XRD) of the samples. The XRD data were taken at temperatures ranging from 10<2θ<80. In surrounding circumstances, to analyze the spectrum's photoluminescence (PL) or the its excitation (PLE), we can utilized the a spex fluorolog-3 spectrofluorometer which has Xe beam ray along with double stimulation monochromators (Instruments S.A.,N J., USA). An incorporating sphere with an internal part covered with Spectralon and a parameter used to measure the spectrofluorometer was used to assess the quantum efficacy (QE) (Horiba Jobin-Yvon Fluorolog 3–22 Tau-3). Liu *et al.* [9] have demonstrated earlier the measuring methodologies and correlating theory [10]–[12]. A hue analyst called Laiko DT-100 along with its CCD detector was used to determine the ***commission international de i'eclairage*** or briefly called CIEchromatic coordinates applied in every specimen. The Hitachi 3010 dual-beam UV-VIS spectrometer paired with an incorporating sphere (Ø 60 mm) whose internal side was covered with barium sulfate **(**$BaSO_4$**)** or Spectralon and polytetrafluoroethylene powder **(**PTFE**)**, scattered reflection spectrum between 200–800 nm were obtained [14]–[16].

2.2. Luminescence properties and energy transfer in $Ca_3Si_2O_4N_2:Eu^{2+}$

The $Ca_3Si_2O_4N_2:Eu^{2+}$exciting and emitting spectrum for various Eu^{2+} concentrations are investigated to determine if it is suitable for using with near UV chip or blue-pumping LED chip. The specimens doped with substantial ratios of Eu^{2+}displayed excitation regions with maximum values at ~289, ~328, ~368, and ~405 nm, which were mostly unresolved regions of the 4*f*65d1 multiplets of the Eu^{2+}exciting conditions. Under optimum stimulation at 330 nm, the material emitted a green spectrum with the greatest at 510 nm. The samples could be stimulated well between 350–400 nm, despite the fact that the optimum excitation was attained at 330 nm. As a result, an n-UV chip with a size of around 380 nm, was chosen for the white LED production. In the wavelength region from 450–650 nm, a large, asymmetrical spectrum was seen in the emitting spectra, which correlates to the permitted $4f65d1 \rightarrow 4f7$ electronic conversions of Eu^{2+}. The significant CaEu-N link's covalency and a strong crystal-field dividing impact attributed to the broad excitation band. The crystal-field dividings of Eu^{2+} were calculated to be 1873021050 cm1 $Ca_3Si_2O_4N_2$. The concentration of the Eu^{2+} dopant grows, according to the Stokes shifts of $Ca_3Si_2O_4N_2$:x%Eu^{2+}(x=0.0025–0.09). The modification in the crystal-field dividing of Eu^{2+} is responsible for the bathochromic change. As a result, the occurrence can be interpreted regarding energy conversion from upper 5*d* levels to smaller 5*d* levels of these ions. The emission energy from 5*d* to the 4*f* ground state decreases as a result, and the emission wavelength moves to a more extended wavelength.

The essential transit distance (R_c) is roughly equivalent to twofold the sphere's radius along with the unit cell volume, according to Blasse [17], [18]:

$$R_c = 2\left[\frac{3V}{4\pi x_c Z}\right]^{\frac{1}{3}} \tag{1}$$

the below formula [19], [20] can be used to represent the emission intensity (I) per activating concentration (x):

$$\frac{I}{x} = \frac{k}{1+\beta(x)^{\theta/3}} \tag{2}$$

when applying phosphor in high-power LEDs, heat stability is something that requires consideration. The PL intensity of the phosphor during operation can be impacted by the temperature of the environment, which is

monitored at a 380 nm wavelength. The activation energy, denoted as Ea, can be calculated using the following equation [21], [22]:

$$\ln\left(\frac{I_o}{I}\right) = \ln A - \frac{E_a}{kT} \quad (3)$$

where the $Ca_3Si_2O_4N_2:Eu^{2+}$ luminescent intensities at ambient temperature and the evaluating temperature are denoted by *Io* and *I*, respectively; *A* and *k* are accordingly an absolute and Boltzman's absolute (8.617×10−5 eV K−1). *Ea* was 0.0687 eV.

The authentic multi-chip white-light LEDs (MCW-LEDs) phosphorus layer is replicated with flattened silicon layers using the LightTools 9.0 application and the Monte Carlo approach [23], [24]. This simulation takes place over two distinct time periods; i) it is critical to establish and create MCW-LED lamp configuration prototypes and optic properties; ii) the optic impacts of phosphor compound are then effectively managed by the $Ca_3Si_2O_4N_2:Eu^{2+}$ concentration variant. We must make some contrast comparisons to observe the impact of $YAG:Ce^{3+}$ and $Ca_3Si_2O_4N_2:Eu^{2+}$ phosphor compounds on the lamps' performance. Double-layer distant phosphorus structure, described as two types of compounds with median correlated color temperatures (CCTs) of 3,000 K, 4,000 K, and 5,000 K, is to be addressed. Figure 1 depicts lamps with conformal phosphorus compound and a median CCT of 8,500 K in detail (a). The modeling of MCW-LEDs without $Ca_3Si_2O_4N_2:Eu^{2+}$ is also recommended. The reflector is 8 mm in the bottom length, 2.07 mm in height, and 9.85 mm in top coat length. The conformal phosphorus compound, which has a precised thickness of 0.08mm, is applied to nine chips. Every LED chip is linked to the reflector cavities by a 1.14 m^2 square core junction and a 0.15 mm height. The blue chips' radiant flux is 1.16 W, with a 453 nm maximum wavelength.

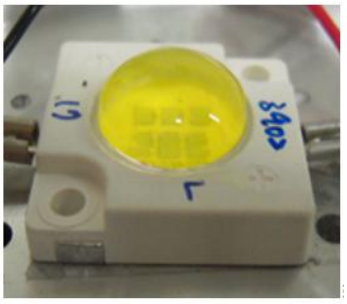

Figure 1. Photograph of WLEDs

3. RESULTS AND ANALYSIS

Figure 2 reveals the reversal shift in the green and yellow phosphorus concentrations. The increase of $Ca_3Si_2O_4N_2:Eu^{2+}$ concentration leads to a decrease in YAG:Ce concentration at 5,700 K (Figure 2(a)) and 8,000 K (Figure 2(b)). This opposition is important to preserve the stability of the WLED at these two CCTs. Moreover, by adjusting the phosphor concentrations, it is possible to regulate the WLED scattering and absorption with two phosphorous layers. As a result, it has an impact on the color standard and illuminating flux capability of WLEDs. The WLEDs color standard is thus determined by the chosen $Ca_3Si_2O_4N_2:Eu^{2+}$ concentration. Since the $Ca_3Si_2O_4N_2:Eu^{2+}$ ratio increased from 2% to 20% wt., the concentration of the yellow phosphor decreased to maintain the median CCTs. This is also true for WLEDs with color temperatures ranging between 5,600 K and 8,500 K.

Figure 3 depicts the $Ca_3Si_2O_4N_2:Eu^{2+}$ green phosphorus concentration impact on the WLEDs transmission spectra. It is feasible to consider the manufacturer's specifications when making decisions. WLEDs that demand good color fidelity can diminish luminous flux by a minor amount. The spectral data have been collected under 5,700 K and 8,500 K, as shown in Figure 3(a) and Figure 3(b), respectively. Clearly, the intensity tendency went up with $Ca_3Si_2O_4N_2:Eu^{2+}$ concentration in two sections of the light spectra: from 420 nm to 480 nm and from 500 nm to 640 nm. This rise in the emission flux may be seen in the two-band emission spectra. When $Ca_3Si_2O_4N_2:Eu^{2+}$ is used, this is a significant outcome. The high heat distant phosphor configuration color homogeneity, particularly, is challenging to manage. This analysis revealed that $Ca_3Si_2O_4N_2:Eu^{2+}$, at both low (6,500 K) and high color temperatures (8,500 K), can improve the WLEDs' color standard. The emitted light flux efficacy of this double-layer distant phosphorus layer was therefore demonstrated in the study in Figure 4. The lumen output was monitored under 5,700 K (Figure 4(a))

and 8,000 K (Figure 4(b)) with the concentration of green $Ca_3Si_2O_4N_2:Eu^{2+}$ ranging from 5% wt. to 15% wt. According to the figures' outcomes, when the $Ca_3Si_2O_4N_2:Eu^{2+}$ concentration is increased, the luminance exhibits enhancement, confirming the stronger luminous emitted of WLEDs using the double-layer distant design with $Ca_3Si_2O_4N_2:Eu^{2+}$ green phosphor.

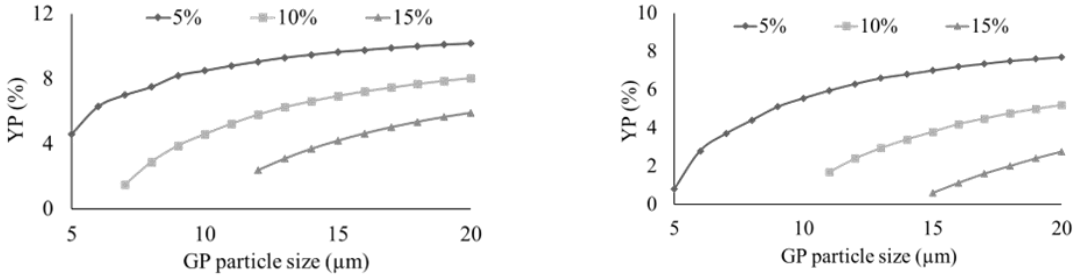

(a) (b)

Figure 2. Modifying the phosphorus concentration to maintain the median CCT: (a) 5,700 K and (b) 8,000 K

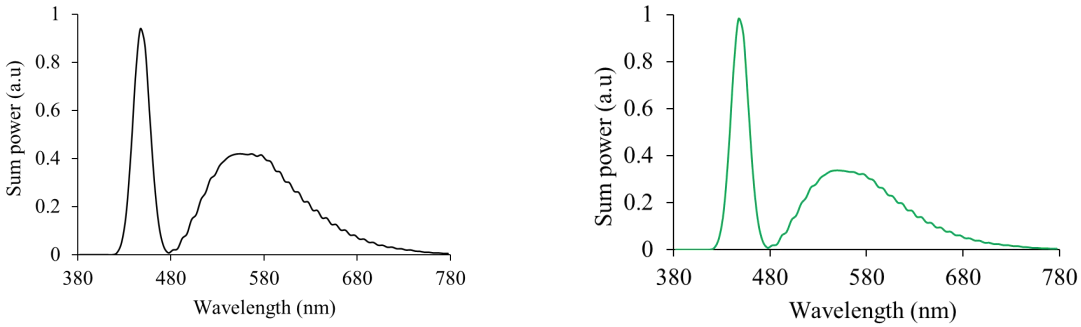

(a) (b)

Figure 3. $Ca_3Si_2O_4N_2:Eu^{2+}$ concentration functions as the WLEDs emission spectrum: (a) 5,700 K and (b) 8,000K

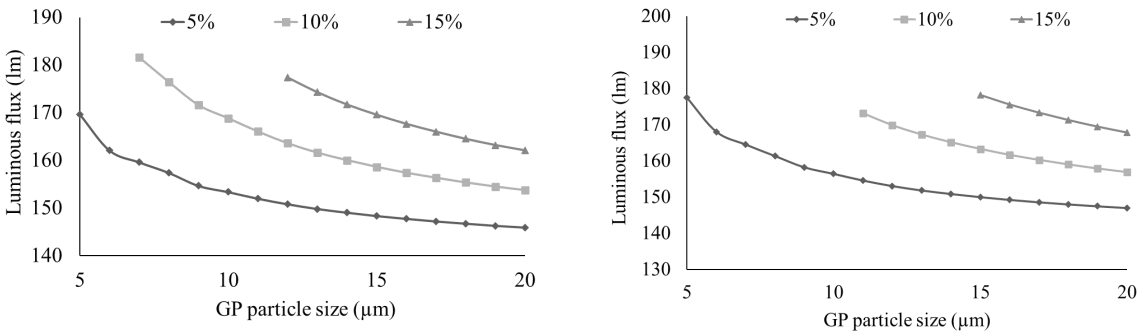

(a) (b)

Figure 4. $Ca_3Si_2O_4N_2:Eu^{2+}$ concentration functions as the WLEDs luminous flux: (a) 5,700 K and (b) 8,000 K

In all two median CCTs, the color divergence was severely decreased by the phosphor $Ca_3Si_2O_4N_2:Eu^{2+}$ concentration, as shown in Figure 5. Notably, the color divergence-correlated color temperatures (D-CCT) at higher CCT of 8,000 K shown a more significant than that at 5,700 K. When the concentration of $Ca_3Si_2O_4N_2:Eu^{2+}$ increases from 2-20 wt., the D-CCT at 5,700 K decreases by 500-520 K (see Figure 5(a)) while that at 8,000 K decreases by ~1,000 K (see Figure 5(b)). The green layer's absorption

is the answer to the situation. When the LED chip's blue light is absorbed, it is converted to green light. The yellow light is absorbed by the $Ca_3Si_2O_4N_2:Eu^{2+}$ particles in complement to the LED chip's blue light. The blue light absorption from the LED chip, however, is more powerful than these two absorbs due to the material's absorption qualities. As a result of the inclusion of $Ca_3Si_2O_4N_2:Eu^{2+}$, the green light element in enhances within WLEDs, improving the color homogeneity indice. Color uniformity is among the most crucial WLED lamp criteria. The greater the color uniformity value, the more expensive WLED white light is. However, the reasonable prices of $Ca_3Si_2O_4N_2:Eu^{2+}$ are a plus. $Ca_3Si_2O_4N_2:Eu^{2+}$ can thus be employed in a variety of applications.

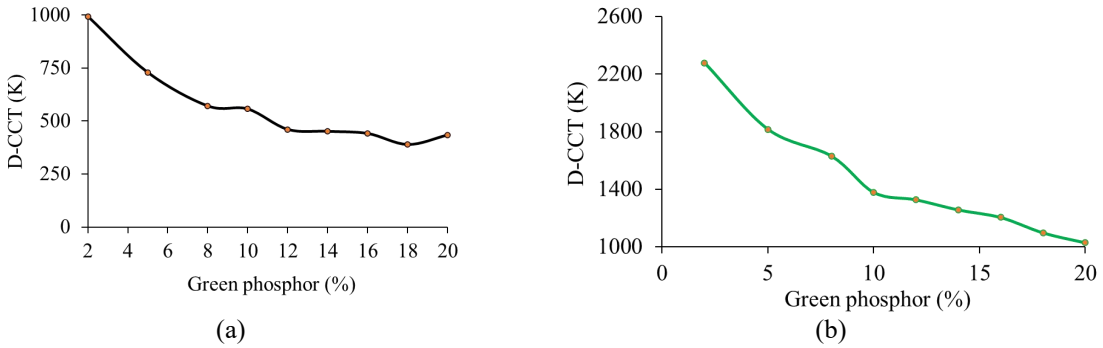

Figure 5. $Ca_3Si_2O_4N_2:Eu^{2+}$ concentration functions as the WLEDs color variation: (a) 5,700 K and (b) 8,000 K

Color uniformity is just a criterion to assess WLED color quality. A WLED cannot claim to have desirable color-quality adequacy if it only has remarkable color homogeneity. As a result, recent researches have developed a color rendering intent and a color quality scale. When light shines on the color rendering indices, it determines the object's exact color. The green light increased volume between three principal colors which are blue, yellow, and green, causing the color imbalance. This has an effect on the WLEDs' color quality, resulting in a decrease in color consistency. The data in Figure 6 show a small decrease in CRI with the inclusion of the distant phosphor $Ca_3Si_2O_4N_2:Eu^{2+}$ layer. Particularly, with 15% wt of $Ca_3Si_2O_4N_2:Eu^{2+}$, CRIs at 5,700 K and 8,000 K, in Figure 6(a) and Figure 6(b) respectively, exhibit the lowest values. Nonetheless, since CRI is merely a flaw in CQS, these are tolerable. In comparison with the CRI, the CQS is more significant and more difficult to attain. CQS is a three-factor index, with the first being the color rendering indices, the second being the user's preference, and the third being the color coordination. With those important factors, CQS is almost a genuine overall assessment of color quality. Figure 7 shows the increase of CQS with the distant phosphor $Ca_3Si_2O_4N_2:Eu^{2+}$ layer presence, which is monitored at 5,700 K (Figure 7(a)) and 8,000 K (Figure 7(b)) with the green phosphor concentration of 5-15% wt. Furthermore, when the $Ca_3Si_2O_4N_2:Eu^{2+}$ concentration is raised, CQS slightly changes when the $Ca_3Si_2O_4N_2:Eu^{2+}$ concentration is under 10% wt. Both CRI and CQS are greatly diminished when $Ca_3Si_2O_4N_2:Eu^{2+}$ concentrations are over 10% wt. owing to extreme color loss as green elements are mostly presented. As a result, if green phosphor $Ca_3Si_2O_4N_2:Eu^{2+}$ is used, proper concentration choice is critical.

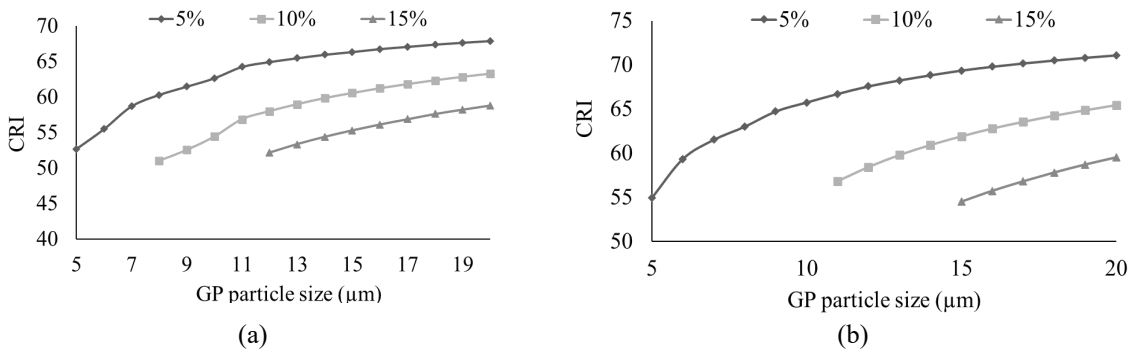

Figure 6. $Ca_3Si_2O_4N_2:Eu^{2+}$ concentration functions as the WLEDs color rendering indice: (a) 5,700 K and (b) 8,000 K

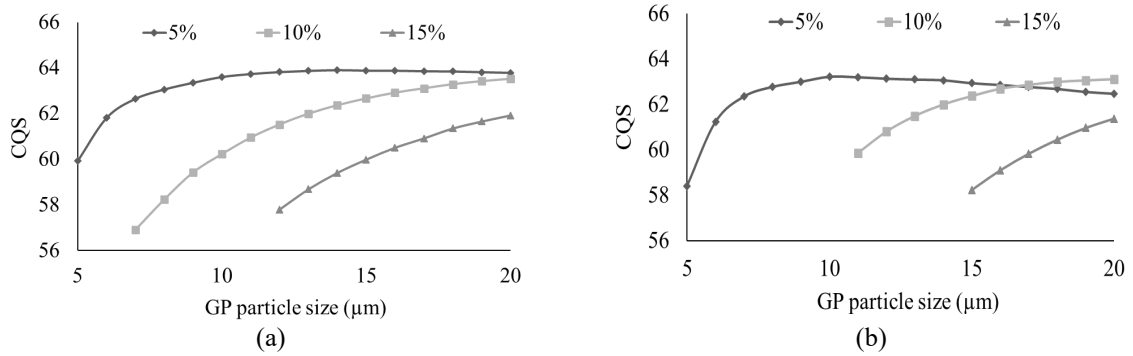

Figure 7. $Ca_3Si_2O_4N_2:Eu^{2+}$ concentration functions as the WLEDs color quality scale: (a) 5,700 K and (b) 8,000 K

4. CONCLUSION

The effect of the green-emitting phosphorus $Ca_3Si_2O_4N_2:Eu^{2+}$ on the double-layer structure's optic properties is discussed in this work. The analysis revealed that $Ca_3Si_2O_4N_2:Eu^{2+}$ is a great option for enhancing color homogeneity depending on Monte Carlo mathematical models. This is true for WLEDs which have a color temperature below 5,000 K as well as those which has a color temperature over 8,500 K. The outcomes of this study have indeed achieved the goal of improving color quality as well as the light flux, which is difficult to do due to the remote structure of phosphor. CRI and CQS, on the other hand, have a slight limitation. As both fall dramatically when the $Ca_3Si_2O_4N_2:Eu^{2+}$ concentration is raised substantially. As a result, the right concentration must be chosen on the basis of the manufacturer's aims. The research has provided a great deal of helpful data for generating higher color homogeneity and luminous flux of WLEDs. A solid-state process was used to effectively manufacture Eu^{2+}-doped nitridosilicate phosphors, $Ca_3Si_2O_4N_2:Eu^{2+}$, for use in wLEDs. The $Ca_3Si_2O_4N_2:Eu^{2+}$ phosphor had high luminous characteristics as well as great heat stability. In $Ca_3Si_2O_4N_2$, the essential conversion gap between Eu^{2+} particles was 30.08. Moreover, the wLEDs color-rendering intent generated in this research is 88.25. As a result, $Ca_3Si_2O_4N_2:Eu^{2+}$ is suggested as a potential solution for wLEDs.

ACKNOWLEDGEMENTS

This study was financially supported by Van Lang University, Vietnam.

REFERENCES

[1] A. Ali *et al.*, "Blue-laser-diode–based high CRI lighting and high-speed visible light communication using narrowband green-/red-emitting composite phosphor film," *Applied Optics*, vol. 59, no. 17, p. 5197, Jun. 2020, doi: 10.1364/AO.392340.
[2] P. Kaur, Kriti, Rahul, S. Kaur, A. Kandasami, and D. P. Singh, "Synchrotron-based VUV excitation-induced ultrahigh quality cool white light luminescence from Sm-doped ZnO," *Optics Letters*, vol. 45, no. 12, p. 3349, Jun. 2020, doi: 10.1364/OL.395393.
[3] F. Brusola, I. Tortajada, I. Lengua, B. Jordá, and G. Peris-Fajarnés, "Parametric effects by using the strip-pair comparison method around red CIE color center," *Optics Express*, vol. 28, no. 14, p. 19966, Jul. 2020, doi: 10.1364/OE.395291.
[4] B. Zhao, Q. Xu, and M. R. Luo, "Color difference evaluation for wide-color-gamut displays," *Journal of the Optical Society of America A*, vol. 37, no. 8, p. 1257, Aug. 2020, doi: 10.1364/JOSAA.394132.
[5] B. K. Tsai, C. C. Cooksey, D. W. Allen, C. C. White, E. Byrd, and D. Jacobs, "Exposure study on UV-induced degradation of PTFE and ceramic optical diffusers," *Applied Optics*, vol. 58, no. 5, p. 1215, Feb. 2019, doi: 10.1364/AO.58.001215.
[6] J. O. Kim, H. S. Jo, and U. C. Ryu, "Improving CRI and scotopic-to-photopic ratio simultaneously by spectral combinations of cct-tunable led lighting composed of multi-chip leds," *Current Optics and Photonics*, vol. 4, no. 3, pp. 247–252, 2020, doi: 10.3807/COPP.2020.4.3.247.
[7] N. A. Mica *et al.*, "Triple-cation perovskite solar cells for visible light communications," *Photonics Research*, vol. 8, no. 8, p. A16, Aug. 2020, doi: 10.1364/PRJ.393647.
[8] Y. C. Liu, J. Zhang, C. K. Tse, C. Zhu, and S.-C. Wong, "General Pathways to Higher Order Compensation Circuits for IPT Converters via Sensitivity Analysis," *IEEE Transactions on Power Electronics*, vol. 36, no. 9, pp. 9897–9906, Sep. 2021, doi: 10.1109/TPEL.2021.3062228.
[9] Y. Wang, G. Xu, S. Xiong, and G. Wu, "Large-field step-structure surface measurement using a femtosecond laser," *Optics Express*, vol. 28, no. 15, p. 22946, Jul. 2020, doi: 10.1364/OE.398400.
[10] M. A. Elkarim, M. M. Elsherbini, H. M. AbdelKader, and M. H. Aly, "Exploring the effect of LED nonlinearity on the performance of layered ACO-OFDM," *Applied Optics*, vol. 59, no. 24, p. 7343, Aug. 2020, doi: 10.1364/AO.397559.
[11] S. Keshri *et al.*, "Stacked volume holographic gratings for extending the operational wavelength range in LED and solar applications," *Applied Optics*, vol. 59, no. 8, p. 2569, Mar. 2020, doi: 10.1364/AO.383577.
[12] H. Yuce, T. Guner, S. Balci, and M. M. Demir, "Phosphor-based white LED by various glassy particles: control over luminous efficiency," *Optics Letters*, vol. 44, no. 3, p. 479, Feb. 2019, doi: 10.1364/OL.44.000479.

[13] H. Q. T. Bui *et al.*, "High-performance nanowire ultraviolet light-emitting diodes with potassium hydroxide and ammonium sulfide surface passivation," *Applied Optics*, vol. 59, no. 24, p. 7352, Aug. 2020, doi: 10.1364/AO.400877.
[14] T. W. Kang *et al.*, "Enhancement of the optical properties of CsPbBr3 perovskite nanocrystals using three different solvents.," *Optics letters*, vol. 45, no. 18, pp. 4972–4975, Sep. 2020, doi: 10.1364/OL.401058.
[15] G. Prabhakar, P. Gregg, L. Rishoj, P. Kristensen, and S. Ramachandran, "Octave-wide supercontinuum generation of light-carrying orbital angular momentum," *Optics Express*, vol. 27, no. 8, p. 11547, Apr. 2019, doi: 10.1364/OE.27.011547.
[16] A. S. Baslamisli and T. Gevers, "Invariant descriptors for intrinsic reflectance optimization," *Journal of the Optical Society of America A*, vol. 38, no. 6, p. 887, Jun. 2021, doi: 10.1364/JOSAA.414682.
[17] G. Granet and J. Bischoff, "Matched coordinates for the analysis of 1D gratings," *Journal of the Optical Society of America A*, vol. 38, no. 6, p. 790, Jun. 2021, doi: 10.1364/JOSAA.422374.
[18] Q. Xu, B. Zhao, G. Cui, and M. R. Luo, "Testing uniform colour spaces using colour differences of a wide colour gamut," *Optics Express*, vol. 29, no. 5, p. 7778, Mar. 2021, doi: 10.1364/OE.413985.
[19] A. Alexeev, J.-P. M. G. Linnartz, K. Arulandu, and X. Deng, "Characterization of dynamic distortion in LED light output for optical wireless communications," *Photonics Research*, vol. 9, no. 6, p. 916, Jun. 2021, doi: 10.1364/PRJ.416269.
[20] R. Fan, S. Fang, C. Liang, Z. Liang, and H. Zhong, "Controllable one-step doping synthesis for the white-light emission of cesium copper iodide perovskites," *Photonics Research*, vol. 9, no. 5, p. 694, May 2021, doi: 10.1364/PRJ.415015.
[21] X. Xi *et al.*, "Chip-level Ce:GdYAG ceramic phosphors with excellent chromaticity parameters for high-brightness white LED device," *Optics Express*, vol. 29, no. 8, p. 11938, Apr. 2021, doi: 10.1364/OE.416486.
[22] I. Fujieda, Y. Tsutsumi, and S. Matsuda, "Spectral study on utilizing ambient light with luminescent materials for display applications," *Optics Express*, vol. 29, no. 5, p. 6691, Mar. 2021, doi: 10.1364/OE.418869.
[23] J. R. Beattie and F. W. L. Esmonde-White, "Exploration of principal component analysis: deriving principal component analysis visually using spectra," *Applied Spectroscopy*, vol. 75, no. 4, pp. 361–375, Apr. 2021, doi: 10.1177/0003702820987847.
[24] Y. Wang *et al.*, "Tunable white light emission of an anti-ultraviolet rare-earth polysiloxane phosphors based on near UV chips," *Optics Express*, vol. 29, no. 6, p. 8997, Mar. 2021, doi: 10.1364/OE.410154.

BIOGRAPHIES OF AUTHORS

Phuc Dang Huu received a physics Ph.D. degree from the University of Science, Ho Chi Minh City, in 2018. Currently, he is a lecturer at the Faculty of Fundamental Science, Industrial University of Ho Chi Minh City, Ho Chi Minh City, Vietnam. His research interests include simulation LEDs material, renewable energy. He can be contacted at email: danghuuphuc@iuh.edu.vn.

Phung Ton That was born in Thua Thien-Hue, Vietnam. He received the B.Sc. degree in electronics and telecommunications engineering (2007) and the M.Sc. degree in electronics engineering (2010) from the University of Technology, Vietnam. He is currently a lecturer at the Faculty of Electronics Technology (FET), Industrial University of Ho Chi Minh City. His research interests are optical materials, wireless communication in 5G, energy harvesting, performance of cognitive radio, physical layer security and NOMA. He can be contacted at email: tonthatphung@iuh.edu.vn.

Phan Xuan Le received a Ph.D. in Mechanical and Electrical Engineering from Kunming University of Science and Technology, Kunming city, Yunnan province, China. Currently, he is a lecturer at the Faculty of Engineering, Van Lang University, Ho Chi Minh City, Viet Nam. His research interests are Optoelectronics (LED), Power transmission and Automation equipment. He can be contacted at email: le.px@vlu.edu.vn.